XIII International Conference on Computational Plasticity. Fundamentals and Applications
COMPLAS XIII
E. Oñate, D.R.J. Owen, D. Peric & M. Chiumenti (Eds)

3D ANALYSIS OF H-M COUPLED PROBLEM WITH ZERO-THICKNESS INTERFACE ELEMENTS APPLIED TO GEOMECHANICS

D. GAROLERA*, J.M. SEGURA†, I. CAROL*, M.R. LAKSHMIKANTHA† AND J. ALVARELLOS‡

* Dept. of Geotechnical Engineering and Geo-Sciences
Universitat Politècnica de Catalunya. BarcelonaTech (UPC)
Campus Nord UPC, 08034 Barcelona, Spain
e-mail: daniel.garolera@upc.edu, ignacio.carol@upc.edu

† Technology Hub - Repsol USA
2455 Technology Forest Blvd
The Woodlands, TX 77381, USA

‡ Repsol. Repsol Technology Centre
Ctra. Extremadura Km. 18
28935 - Móstoles, Spain

Key words: zero-thickness interface, hydraulic fracture, hydro-mechanic coupling

Abstract. In spite of the significant developments seen in recent years, numerical modeling of Hydraulic Fracturing still poses major challenges due to the strong coupling between fluid flow and crack development, which is itself a strongly non-linear problem. The objective of this paper is to show advances in a line of work started by Segura and Carol [1], on the modeling of coupled H-M discontinuities via zero-thickness interface elements. In particular, this paper is focused on the 3D applications of the approach, and the results obtained are compared to the existing GDK and PKN analytical solutions. For the comparison, two 3D models are described: a plate model for the GDK, and a block model for the PKN. In order to improve de modelling, both models are run with interfaces equipped with realistic non-linear material laws based on fracture energy. Results obtained show a good agreement with both analytical and numerical results.

1 INTRODUCTION

Advanced Geo-mechanical modelling involves the treatment of geological discontinuities. In the approach described in this paper, zero-thickness interface elements of the Goodman type [2] are considered for this purpose. Those elements can also be used for

representing the fluid flow and the coupled hydro-mechanical problem [1]. The technique consists of inserting interface elements in between standard elements to allow jumps in the solution fields. For the mechanical problem, their kinematic constitutive (strain-type) variables are relative displacements, and the corresponding static (stress-type) variables are stress tractions. The relationship between variables is controlled via a fracture-based constitutive law with elasto-plastic structure [3]. Concerning the hydraulic problem, the interface formulation includes both the longitudinal flow (with a longitudinal conductivity parameter strongly dependent on the fracture aperture, cubic law), as well as and the transversal flow across the element (and an associated localized pressure drop, with the corresponding transversal conductivity parameter).

The formulation presented in this paper is the 3D extension of recent work presented by the authors [4] which was verified first by comparison to existing analytical and numerical solutions for the propagation of a single hydraulic fracture [5]. The current implementation is compared to two examples: the first one consists of a horizontal layer of 1m of thickness with a line-like distributed flow injection, with the purpose of simulating as close as possible the standard GDK conditions model. The second case consists of a cubic block of 80m side composed of the same horizontal thin layer surrounded by thick overburden and underburden layers and contact interfaces, the results of which are compared with the classical PKN solution. General good agreement is observed in both cases between the numerical results and both analytical solutions. The comparisons also motivates a discussion on the boundary conditions implicit in those classical solutions.

2 HYDROMECHANICAL FORMULATION FOR ZERO-THICKNESS INTERFACE ELEMENTS

Present work follows the definition of zero-thickness interface element proposed by [6]. The main characteristic of this special element is that one of its dimensions is collapsed. Therefore the integration is reduced in one order, line and surface integrations for 2D and 3D respectively. For this purpose, nodal unknowns are transformed into midplane variables which represent variations (jumps or drops) of field variables. Midplane variables are expressed in terms of the local orthogonal coordinates system, presented in section 2.1. Then, the HM formulation is shown in section 2.2.

2.1 Zero-thickness variables

The nodal variables in a hydro-mechanical problem include the nodal displacements ($\mathbf{u}^e$) and the nodal fluid pressures ($\mathbf{p}^e$). The nodal (absolute) displacements are transformed into normal (r_n) and shear (r_{l_1}, r_{l_2}) relative displacements, which have the meaning of displacements jumps across the discontinuity. The other variable, fluid pressure, is transformed into two components, the average pressure ($\bar{p}_{\mathbb{J}}$) and the pressure drop ($\check{p}_{\mathbb{J}}$), across the discontinuity. A description of these variables and their conjugates is provided in the following paragraphs.

The relative displacement at a mid-plane point "ξ" of the discontinuity is denoted as:

$$\mathbf{r}_{\mathbb{J}}\big|_{\xi} = \begin{pmatrix} r_n & r_{l_1} & r_{l_2} \end{pmatrix}\big|_{\xi}^{\top} \tag{1}$$

where r_n is the normal component and the $r_{l_{(*)}}$ are the tangential components. These relative displacements and the corresponding stress variables are depicted in figure 1.

The relation between relative displacements and nodal displacements is given by the the following expressions:

$$\begin{aligned} \mathbf{r}_{\mathbb{J}}\big|_{\xi} &= \mathbf{R}\ \mathbf{N}_{\mathbb{J}}{}^{u}\big|_{\xi}\, \mathbf{T}_{\mathbb{J}}{}^{u}\, \mathbf{u}_e = \\ &= \mathbf{B}_{\mathbb{J}}\big|_{\xi}\, \mathbf{u}_e \qquad (2) \\ \mathbf{B}_{\mathbb{J}}\big|_{\xi} &= \mathbf{R}\ \mathbf{N}_{\mathbb{J}}{}^{u}\big|_{\xi}\, \mathbf{T}_{\mathbb{J}}{}^{u} \qquad (3) \end{aligned}$$

where $\mathbf{R}$ is the rotation matrix that transforms vector components into local orthogonal axes, $\mathbf{N}_{\mathbb{J}}{}^{u}$ is matrix of nodal shape functions evaluated at integration position ξ, and $\mathbf{T}_{\mathbb{J}}{}^{u}$ is the "transport" matrix, which generates the difference between bottom and top face of interface element. Then, $\mathbf{B}_{\mathbb{J}}$ matrix is defined in analogy to continuum description.

The matrix of nodal shape functions is defined in eq. 4, where index m represents the number of nodes at midplane, which is equivalent to half of the number pf nodes of the element node (n). Index k represents the number of mechanical degrees of freedom per node.

$$\mathbf{N}_{\mathbb{J}}{}^{u}\big|_{\xi} = \begin{pmatrix} N_1^u\big|_{\xi} & N_2^u\big|_{\xi} & \cdots & N_m^u\big|_{\xi} \end{pmatrix} \otimes \mathbf{I}_k \tag{4}$$

The mechanical transport matrix for the mechanical problem is defined as:

$$\mathbf{T}_{\mathbb{J}}{}^{u} = \begin{pmatrix} -\mathbf{I}_m & \mathbf{I}_m \end{pmatrix} \tag{5}$$

The conjugate variables to the relative displacements are the stress tractions at the discontinuity mid-plane ($\boldsymbol{\sigma}_{\mathbb{J}}$), which, for specific point ξ of that surface, may be expressed as:

$$\boldsymbol{\sigma}_{\mathbb{J}}\big|_{\xi} = \begin{pmatrix} \sigma_n & \tau_1 & \tau_2 \end{pmatrix}\big|_{\xi}^{\top} \tag{6}$$

where σ_n is the normal stress and τ_* are the tangential components.

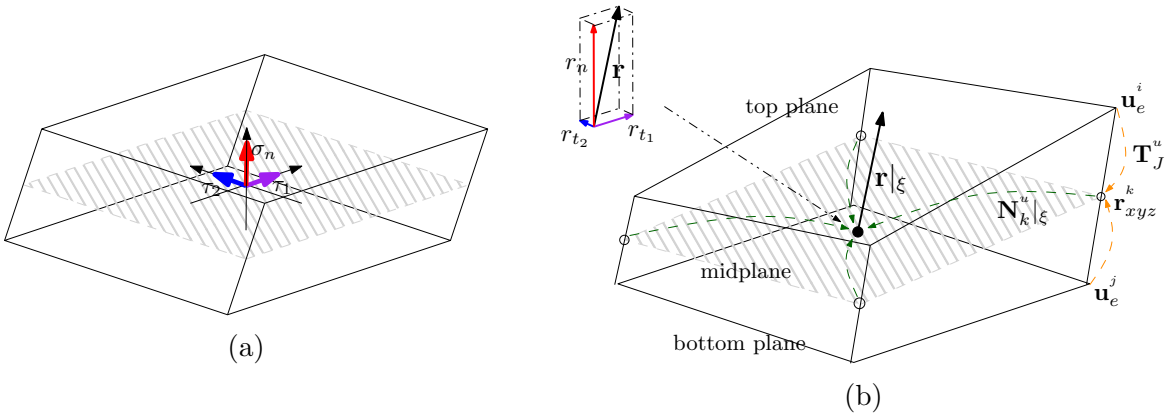

Figure 1: Stresses and relative displacements of zero-thickness interface element: 1a) stress and 1b) the relative displacements.

The average fluid pressure ($\bar{p}_{\mathbb{J}}$) at a given point "ξ" of the discontinuity is obtained as the average between bottom and top fluid pressures and it can be expressed as:

$$\bar{p}_{\mathbb{J}}\big|_\xi = {\mathbf{N}_{\mathbb{J}}}^p\big|_\xi^\top \, {\mathbf{T}_{\mathbb{J}_l}}^p \, \mathbf{p}_e \tag{7}$$

$${\mathbf{N}_{\mathbb{J}}}^p\big|_\xi = \begin{pmatrix} N_1^p & N_2^p & \cdots & N_m^p \end{pmatrix}\Big|_\xi \otimes \mathbf{I}_1 \tag{8}$$

$${\mathbf{T}_{\mathbb{J}_l}}^p = \frac{1}{2}\begin{pmatrix} \mathbf{I}_m & \mathbf{I}_m \end{pmatrix} \tag{9}$$

The fluid pressure drop at the same point is given by the difference between top and bottom fluid pressures at element nodes:

$$\check{p}_{\mathbb{J}}\big|_\xi = {\mathbf{N}_{\mathbb{J}}}^p\big|_\xi^\top \, {\mathbf{T}_{\mathbb{J}_t}}^p \, \mathbf{p}_e \tag{10}$$

$${\mathbf{T}_{\mathbb{J}_t}}^p = \begin{pmatrix} -\mathbf{I}_m & \mathbf{I}_m \end{pmatrix} \tag{11}$$

2.2 Finite element method formulations

This section describes the weak form of the equilibrium/continuity used for the implementation of zero-thickness interface elements. This equations are obtained from the application of Virtual work Principle. and the details can be found in [1]. The notation follows the terminology given in [7].

$$\int_{\Omega_j} {\mathbf{B}_{\mathbb{J}}}^\top \, {\boldsymbol{\sigma}_{\mathbb{J}}}' \, d\Omega_j + \mathbf{Q}_{\mathbb{J}} \, \mathbf{p}_e = {\mathbf{f}_{\mathbb{J}}}^u \tag{12}$$

$$\mathbf{H}_{\mathbb{J}} \, \mathbf{p}_e + \mathbf{S}_{\mathbb{J}} \frac{\partial \, \mathbf{p}_e}{\partial t} + \mathbf{Q}_{\mathbb{J}} \frac{\partial \, \mathbf{u}_e}{\partial t} + \mathbf{g}_{\mathbb{J}} = \mathbf{f}_e^p \tag{13}$$

in which $\mathbf{Q}_{\mathbb{J}}$ is the coupling matrix, $\mathbf{H}_{\mathbb{J}}$ the diffusion matrix, $\mathbf{S}_{\mathbb{J}}$ the storage matrix and $\mathbf{g}_{\mathbb{J}}$ is the gravity term.

$$\mathbf{Q}_{\mathbb{J}} = \mathbf{T}_{\mathbb{J}}{}^{u\top} \int_{\Omega_j} \mathbf{N}_{\mathbb{J}}{}^{u\top} \mathbf{R}^{\top} \alpha_j \, \mathbf{m}_{\mathbb{J}} \mathbf{N}_{\mathbb{J}}{}^{p\top} \, d\Omega_j \, \mathbf{T}_{\mathbb{J}_l}{}^{p} \tag{14}$$

$$\begin{aligned} \mathbf{H}_{\mathbb{J}} &= \mathbf{H}_{\mathbb{J}_t} + \mathbf{H}_{\mathbb{J}_l} = \\ &= \mathbf{T}_{\mathbb{J}_t}{}^{p\top} \left(\int_{\Omega_j} \mathbf{N}_{\mathbb{J}}{}^{p\top} \check{K}_t \mathbf{N}_{\mathbb{J}}{}^{p\top} \, d\Omega_j \right) \mathbf{T}_{\mathbb{J}_t}{}^{p} + \\ &+ \mathbf{T}_{\mathbb{J}_l}{}^{p\top} \left(\int_{\Omega_j} \frac{\partial \, \mathbf{N}_{\mathbb{J}}{}^{p\top}}{\partial \Omega_j} \frac{T_l}{\gamma_f} \frac{\partial \, \mathbf{N}_{\mathbb{J}}{}^{p\top}}{\partial \Omega_j} \, d\Omega_j \right) \mathbf{T}_{\mathbb{J}_l}{}^{p} \end{aligned} \tag{15}$$

$$\mathbf{S}_{\mathbb{J}} = \mathbf{T}_{\mathbb{J}_l}{}^{p\top} \left(\int_{\Omega_j} \mathbf{N}_{\mathbb{J}}{}^{p\top} \frac{1}{M_j} \mathbf{N}_{\mathbb{J}}{}^{p} \, d\Omega_j \right) \mathbf{T}_{\mathbb{J}_l}{}^{p} \tag{16}$$

$$\mathbf{g}_{\mathbb{J}} = \mathbf{T}_{\mathbb{J}_l}{}^{p\top} \left(\int_{\Omega_j} \frac{\partial \, \mathbf{N}_{\mathbb{J}}{}^{p\top}}{\partial \Omega_j} T_l \frac{\partial z_{mp}}{\partial l} \, d\Omega_j \right) \tag{17}$$

where α_j is the Biot's coefficient, $\mathbf{m}_{\mathbb{J}} = (1 \; 0 \; 0)^{\top}$, $\check{K}_t$ the transversal conductivity, T_l the longitudinal transmissivity, γ_f the specific fluid weight and M_j the Biot's modulus.

3 STUDY OF A SINGLE H-M FRACTURE IN 3D

This section describes the results of the 3-D analysis of a single fracture. The calculations performed include two different cases, and whenever possible, the results are compared with previous existent 2D analytical and numerical solutions. The main objective of the examples selected is to demonstrate the applicability of 3D analysis with zero-thickness interface elements to HF problems.

The first 3D example models a horizontal layer of 1m of thickness with a line-like distributed flow injection, with the purpose of simulating as close as possible the conditions of the standard GDK formula [8]. The second example also represents a horizontal layer of 1m of thickness, but in this case embedded in a block of 80m side. Same as in the first example, a line-like distributed flow injection is imposed along the central 1m section of the vertical fracture mouth, with the purpose of simulating as close as possible the conditions of the standard PKN-model [8].

3.1 Analytical solutions GDK and PKN

The classical solutions for 2D planar fractures, GDK and PKN, are summarized in this section.

3.1.1 GDK (Geertsma De Klerk Khristianovich)

The GDK model is applicable when the fracture height is greater than the fracture length ($H > H$, see fig.2a) [8]. The main assumptions implicit in this model are: *a*) the fracture width is proportional to its fracture length ($W \propto L$) *b*) the fracture height is constant *c*) the fracture has an elliptical cross-section in the horizontal plane *d*) the cross section in the vertical plane is rectangular (fracture width is constant along its height)

The geometry of the fracture is shown in figure 2a. The comparison with numerical results is made in terms of the evolution of the crack mouth opening displacement (CMOD), which for the GDK model can be expressed in closed form as:

$$CMOD = 1.87 \left(\frac{(1-\nu)\,\mu Q_0^3}{G} \right)^{\frac{1}{6}} t^{\frac{1}{3}} \tag{18}$$

where G is the shear modulus, Q_0 is the flow injected, ν the Poissons ratio, μ the kinematic viscosity and t the time.

3.1.2 PKN (Perkins Kern Nordgren)

This model is used when the fracture length is much greater than the fracture height ($L >> H$) [8]. The main assumptions of this model are: *a*) every vertical cross section acts independently. *b*) the PKN model neglects the effect of fracture tip and fracture mechanics and focuses on fluid flow and the corresponding pressure gradients *c*) the height of the vertical fracture is constant and does not exceed the pay zone *d*) the cross section of the fracture is assumed to be elliptical. *e*) at any cross section the maximum width is proportional to the net pressure at that point and independent of the width at the pay point.

The geometry of the fracture is shown in figure 2b. The evolution of crack-mouth opening displacement (CMOD), which is again used to compare the numerical results, is given in this model by the following formula:

$$CMOD = 2.5 \left(\frac{(1-\nu)\,\mu Q_0^2}{GH} \right)^{\frac{1}{5}} t^{\frac{1}{5}} \tag{19}$$

where H is the fracture height.

3.2 Model definition

3.2.1 Material properties

The material properties that have been used in the simulations are given below. For the continuum elements, the material is assumed elastic isotropic material is assumed. Regarding the hydraulic behaviour, the material is taken as practically impervious as it corresponds to the assumptions of the PKN solution. All parameters are displayed in table 1.

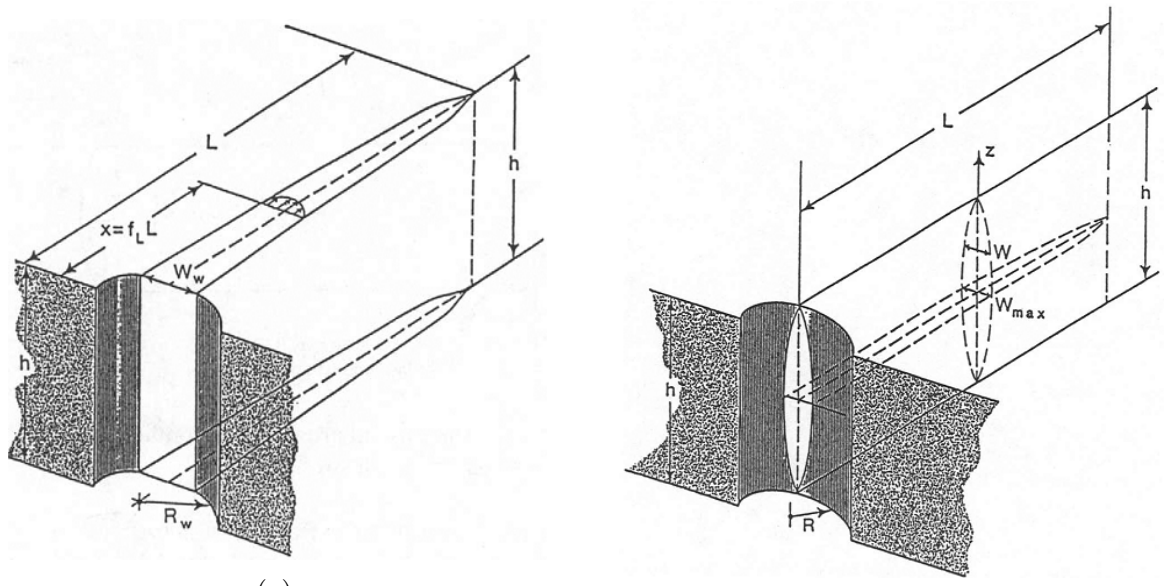

Figure 2: Model geometry for a 2D fracture; a) the GDK constant height fracture model; b) fracture plane. [8]

Table 1: Material properties of continuum.

E (Youngs modulus	14400	MPa
ν (Poissons ratio)	0.2	-
K (hydraulic conductivity)	10^{-15}	m/s
Ks (solid compressibility)	36000	MPa
α (Biot coef.)	1.0	-

For the mechanical behaviour of the interface elements, normal and shear stiffness are assigned high values. These parameters may be understood as penalty coefficients with high values in order to avoid excessive unrealistic elastic deformations at the interfaces. Therefore, in practice the resulting deformation of the fractures can be assumed to represent almost exclusively the inelastic behaviour, that is, crack opening and shear slip. The constitutive model used for the fractures is the elastoplastic constitutive formulation with fracture energy-based evolution laws described in detail in [3]. Low values of strength (tensile strength and cohesion) are selected in order to simulate existing fractures with very low or practically null cohesion [5]. The hydraulic behaviour of the interface is controlled by the so-called cubic law. The summary of interface parameters is shown in table 2.

Table 2: Material properties of interfaces.

K_n	1000000	MPa/m
K_{t_1} and K_{t_2}	1000000	MPa/m
ξ (tensile strength)	0.002	MPa
$\tan(\phi)$ (friction angle)	0.2 (11.3°)	
c (cohesion)	0.01	MPa
G_f^I (fracture energy mode I)	0.001	MPa×m
G_f^{IIa} (fracture energy mode IIa)	0.01	MPa×m
T_{l_0} (initial longitudinal transmissivity)	0.0	m^2/s
K_t^p (transversal conductivity)	1.0	1/s
α Biot coef.	1.0	
M Biot modulus	10000000000	

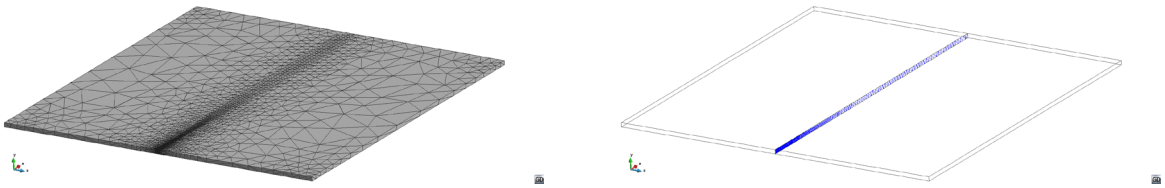

(a) (b)

Figure 3: Model mesh; a) entire domain (continuum elements); b) fracture plane.

3.2.2 Model geometry

GDK As described before the model geometry of GDK case is composed by a 3D layer of 1m thickness, as depicted in figure 3. The objective of this case is to reproduce in 3D one case already run with 2D analysis [4], in order to compare the results for validation.

A fracture plane is placed vertically in the middle of the model. Figure 3 shows the linear mesh used for the simulations (8165 nodes), with diagram a) showing the continuum mesh (30545 tetrahedrons) and diagram b) the fracture plane, which is composed of planar interface elements (1331 triangular zero-thickness interface elements). Due to the high gradients at the injection line, a finer discretization is used along this line.

PKN The 3-D simulation of this case involves a cubic block of 80 m side with an embedded horizontal layer in the middle. Zero-thickness interface elements are pre-inserted over the part of the vertical mid-plane that belongs to the middle layer, which constitutes

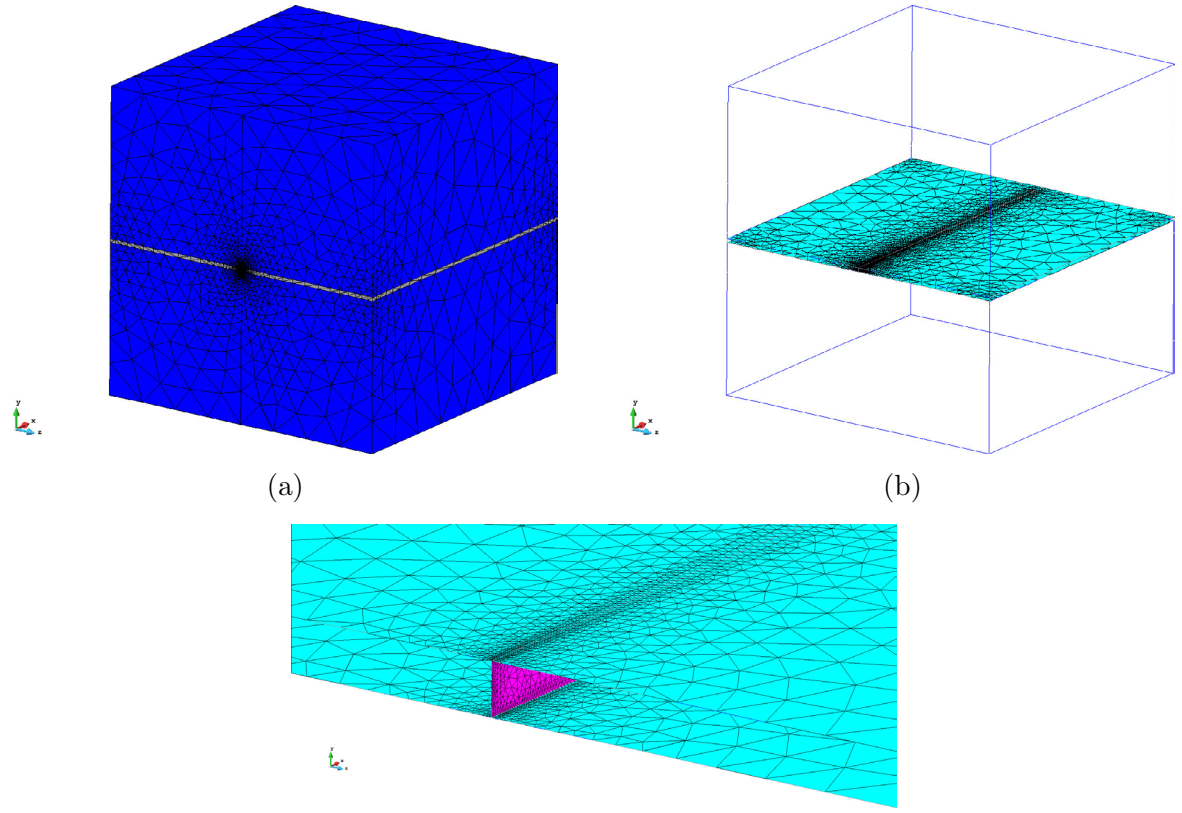

Figure 4: Model mesh; a) entire domain (continuum elements); b) fracture planes; and c) detail of the pre-established fracture surfaces at the crack mouth (interfaces).

the potential fracture path. A second set of interface elements are located at each contact between the horizontal layers. The geometry of the model is illustrated in figure 4, where a linear mesh of 24198 nodes is used for the simulations. Figure 4a shows the continuum mesh (109033 tetrahedra) and figure 4b shows the fracture planes and the layer discontinuities, which are composed of planar interface elements (9015 triangular zero-thickness interface elements). Due to the high gradients at the injection point, a finer discretization is used near the injection point (figure 4c).

In this analysis, the horizontal interface plane is assumed to be elastic with $K_n = 1000$ GPa/m and $K_t = 25$ GPa/m.

3.2.3 Loading and boundary conditions

The loading and boundary conditions are applied in two steps (figure 5):

- A distributed compressive load of 1.0 Mpa is applied over the entire outer boundary in order to simulate the in-situ initial stress. Hydraulic pore pressure is assumed to

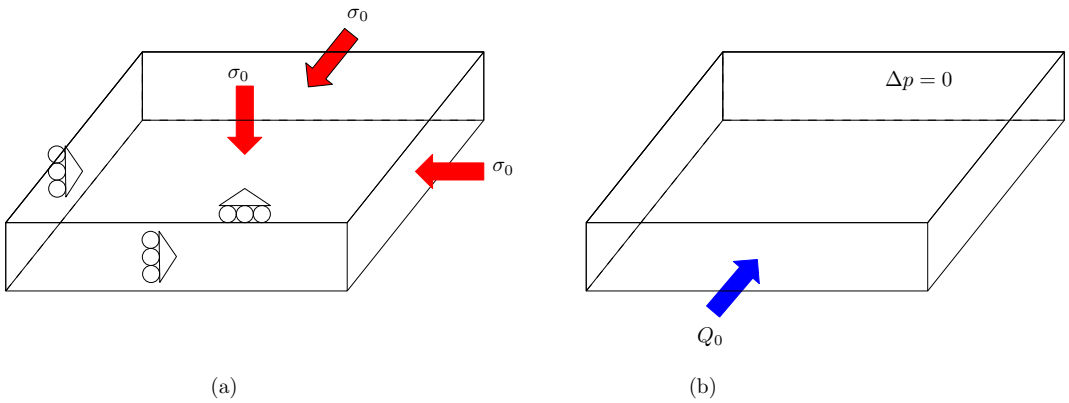

Figure 5: Boundary conditions for both mechanical and hydraulic problems each step of the analysis.

be zero, and the simulation is run in steady state conditions.

- During the injection step, the fluid flow is injected at the fracture mouth. Due to the interest to simulate conditions as close as possible to the 2D model, the flow rate is imposed all along the fracture mouth line, at the constant value of 0.0001 $m^3/s/m$ and during a time step of 25s. The boundary conditions on the face at the opposite side of the injection correspond to a zero fluid pressure increment, while zero flow is assumed for the rest of the domain boundaries.

3.3 Results

Figure 6 shows the evolution of the crack mouth opening displacement (CMOD) and the evolution of the crack mouth pressure (CMP), for the 25 first seconds of injection. For the GDK case (fig.6a) the results obtained with the 3D analysis assuming plane strain conditions are in perfect agreement with those results obtained with both analytical (eq.18) and numerical solutions in 2D, [5] and [4].

Concerning the PKN case, the results provided by the three-layer analysis give a general good agreement with the PKN formula. Figure 6b shows the crack mouth opening displacement evolution (CMOD), which turns out slightly lower than the prediction via original PKN expression (eq.19).

Finally the distribution of fluid pressure for 25s of injection is presented in figure 7. In this figure, the pressure values are represented on the deformed shape of the fracture, which in both cases turns out to be in good agreement with the shapes assumed in the GDK and PKN formulas.

4 CONCLUDING REMARKS

A methodology for 3D analysis of hydraulic fracture is presented which is based on the use of zero-thickness interface elements with full H-M coupling approach. In this

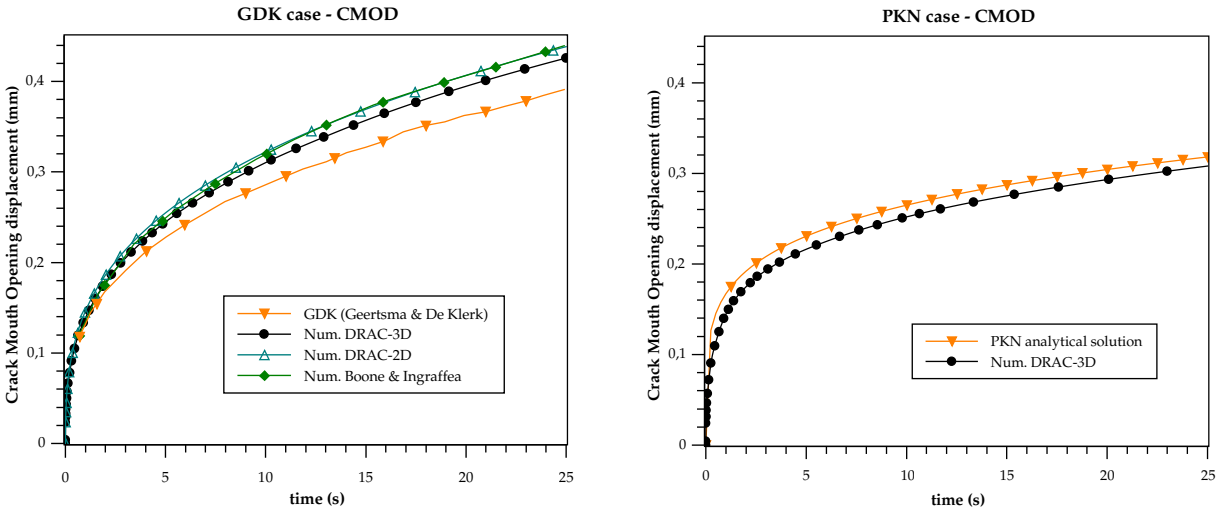

(a) (b)

Figure 6: Curves of Crack Mouth Opening Displacement (CMOD) evolution with time, for the two-dimensional GDK formula problem (left), and for the 3D PKN formula problem(right). The numerical results are all obtained in 3D.

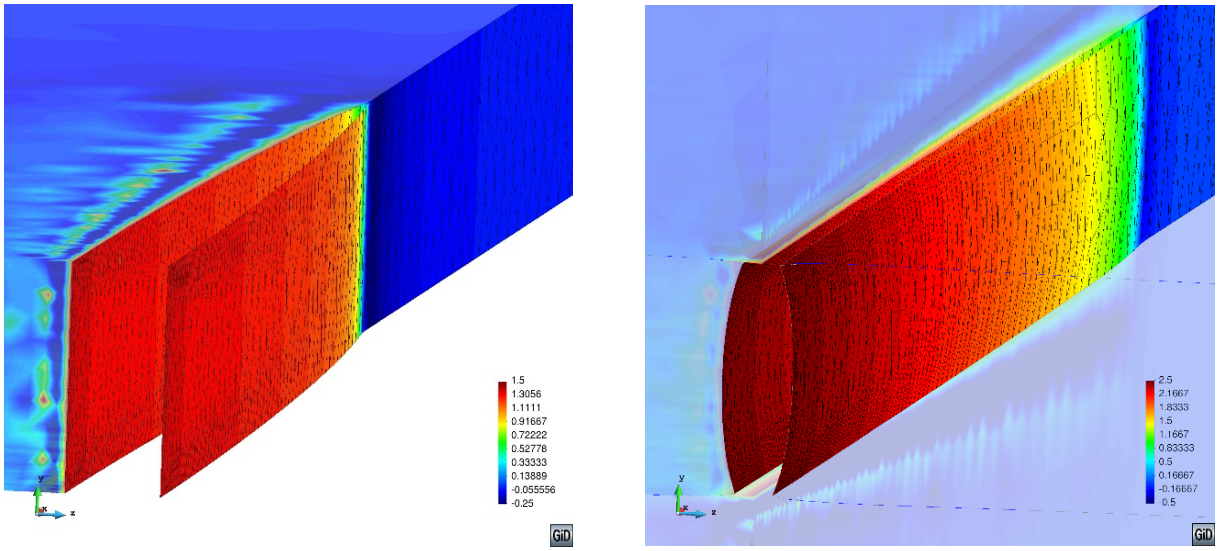

(a) (b)

Figure 7: Fluid pressure distribution after stopping injection (25 seconds): 3D numerical results obtained for the 2D GDK formula (left), and 3D PKN formula (right). Colors represent pressure intensities depicted over deformed mesh (with x1000 magnification factor).

paper, the examples presented involve single fracture in 3D in order to compare with existing closed-form analytical formulas GDK and PKN. The first one assumes plane strain conditions, and the comparison includes also results obtained previously with the same approach in 2D. The second on (PKN) assumes a given fracture height with elliptical section. The 3D results presented in this paper are in good agreement with the formulas and with previous 2D numerical solutions, and therefore they seem to confirm that the approach described provides a good, realistic tool for the numerical representation of strongly H-M coupled problems such as hydraulic fracture.

5 ACKNOWLEDGEMENTS

The work was partially supported by research grants BIA2012-36898 from MEC (Madrid), which includes FEDER funds, and 2014SGR-1523 from Generalitat de Catalunya (Barcelona). The support from REPSOL for this research is also greatfully acknowledged.

REFERENCES

[1] Segura, J.M. and Carol, I. Coupled HM analysis using zero-thickness interface elements with double nodes. Part I: theoretical model, and Part II: verification and application. *Int. J. Numer. Analyt. Meth. in Geomechanics*, 32(18):20832123 (2008).

[2] Gens, A., Carol, I. and Alonso, E. A constitutive model for rock joints formulation and numerical implementation. *Computers and Geotechnics*, 9, 3-20, (1990).

[3] Carol, I, Prat, P. and López, C.M., A normal/shear cracking model. Application to discrete crack analysis. *ASCE J. Engrg. Mech.*, Vol 123(8), p. 765-773 (1997).

[4] Garolera D., Aliguer, I., Segura, J.M., Carol, I., Lakshmikantha, M.R. and Alvarellos, J., Hydro-mechanical coupling in zero-thickness interface elements, formulation and applications in geomechanics. *Proceedings of EUROCK 2014*, CRC Press, p. 1379-1384. (2014).

[5] Boone,T.J. and Ingraffea, A.R., A numerical procedure for simulation of hydraulic-driven fracture propagation in poroelastic media *Int. J. for Numer. Analyt. Meth. in Geomechanics*, 14, 27-47, (1990).

[6] Goodman, R. E. and Taylor, R. L. and Brekke, T. L. A model for the mechanics of jointed rock. *Journal of the Soil Mechanics and Foundation Division*, 94, 637-659, (1968).

[7] Zienkiewicz, O.C. and Taylor, R.L. *The finite element method.* McGraw Hill, Vol. I., (2000)

[8] Yew, C.H. *Mechanics of hydraulic fracturing.* Gulf Publishing Co., Houston, (1997).